

Precision predictions for Z' -production at the CERN LHC: QCD matrix elements, parton showers, and joint resummation

Benjamin Fuks^{a,b}, Michael Klasen^{b,*}, Fabienne Ledroit^b, Qiang Li^{b,c}, and Julien Morel^b

^a *Physikalisches Institut, Albert-Ludwigs-Universität Freiburg,
 Hermann-Herder-Straße 3, D-79106 Freiburg i.Br., Germany*

^b *Laboratoire de Physique Subatomique et de Cosmologie,*

Université Joseph Fourier/CNRS-IN2P3/INPG, 53 Avenue des Martyrs, F-38026 Grenoble, France

^c *Institut für Theoretische Physik, Universität Karlsruhe, Postfach 6980, D-76128 Karlsruhe, Germany*

(Dated: February 9, 2022)

We improve the theoretical predictions for the production of extra neutral gauge bosons at hadron colliders by implementing the Z' bosons in the MC@NLO generator and by computing their differential and total cross sections in joint p_T and threshold resummation. The two improved predictions are found to be in excellent agreement with each other for mass spectra, p_T spectra, and total cross sections, while the PYTHIA parton and “power” shower predictions usually employed for experimental analyses show significant shortcomings both in normalization and shape. The theoretical uncertainties from scale and parton density variations and non-perturbative effects are found to be 9%, 8%, and less than 5%, respectively, and thus under good control. The implementation of our improved predictions in terms of the new MC@NLO generator or resummed K factors in the analysis chains of the Tevatron and LHC experiments should be straightforward and lead to more precise determinations or limits of the Z' boson masses and/or couplings.

I. INTRODUCTION

Despite its impressive phenomenological success, the Standard Model (SM) of particle physics is widely believed to suffer from a variety of conceptual deficiencies. In particular, it provides no fundamental motivation why the strong and electroweak interactions should be described by three different gauge groups, i.e. $SU(3)$, $SU(2)$, and $U(1)$. Grand Unified Theories (GUTs) allow for a unification of these groups within a simple Lie group such as $SU(5)$, $SO(10)$, or E_6 . Depending on the rank of the unifying group, one or several extra neutral gauge (Z') bosons appear when the unification group is broken to the SM at higher scales, exhibiting the existence of additional $U(1)$ symmetries [1]. Anomaly cancellations and gauge invariance of quark and lepton Yukawa couplings impose a number of restrictions on these additional symmetries. Viable families of models, that are consistent with constraints coming from the CERN LEP collider, include those based on the $B - L$ and $SO(10)$ symmetries and, provided that fermion mass generation is not restricted to the SM Higgs mechanism and new charged fermions are allowed, also those inspired by E_6 [2].

If the extra Z' -bosons couple to quarks and leptons with approximately SM strength and if their mass is not too large, they will be produced at current and future hadron colliders and can be easily detected through their leptonic decay channels. The search for these particles occupies therefore an important place in the experimental programs of the Fermilab Tevatron and the CERN LHC. For example, the CDF collaboration has searched the Tevatron Run II data for Z' -bosons in the e^+e^- decay channel, using the di-electron invariant mass and angular distributions and setting lower mass limits of 650 to 900 GeV for a large variety of models [3]. Similar constraints come from electroweak precision fits and di-fermion production at LEP2 [4]. Within the ATLAS collaboration, the discovery reach in $Z' \rightarrow e^+e^-$ decays has recently been analyzed [5] for the four classes of models defined in Ref. [2]. The CMS collaboration has claimed a discovery reach of masses between 3.4 and 4.3 TeV for the $Z' \rightarrow \mu^+\mu^-$ decay channel and an integrated luminosity of 100 fb^{-1} [6].

The currently available simulations for the LHC experiments rely completely on the PYTHIA Monte Carlo (MC) generator [7], which is based on leading order (LO) QCD matrix elements, parton showers, and the Lund string hadronization model. It includes the full interference structure of new Z' -bosons with Drell-Yan photon and SM Z -boson exchange, and the above-mentioned phenomenologically viable models can easily be implemented [8]. The description of the transverse-momentum (p_T) spectrum of the produced vector-boson can be improved by matching the parton shower to the hard emission of an extra parton [9], but the overall normalization of the theoretical cross

*klasen@lpsc.in2p3.fr

section remains subject to large higher-order corrections and scale uncertainties. The CDF collaboration has therefore chosen to renormalize the generated Monte Carlo events with a correction (K) factor in each invariant mass bin to the next-to-next-to-leading order (NNLO) cross section [10]. However, this procedure does not lead to a correct description of the transverse-momentum spectrum. Note also that in principle the LO cross section no longer factorizes at NNLO, i.e. the K -factors for Drell-Yan and Z' production need no longer to be equal [2].

Here, we report on the implementation of extra Z' -bosons in the next-to-leading order (NLO) Monte Carlo generator MC@NLO [11], allowing to match the complete NLO matrix elements with the parton shower and cluster hadronization model of the Monte Carlo generator HERWIG [12]. Since the LO cross section still factorizes completely at NLO, this requires the implementation of the Z' -boson mass, decay width, propagator, and couplings in MC@NLO, together with the full interference with Drell-Yan photon and SM Z -boson exchanges. As was the case for PYTHIA, the emission of one additional hard parton has previously been matched to the HERWIG parton shower, albeit for SM vector-boson production only [13]. As an alternative, the CKKW formalism [14] for the matching of hard real emissions has been implemented in both PYTHIA and HERWIG for SM vector-boson production with the result that the three different matching formalisms were found to vary systematically in a significant way and to depend in addition strongly on the matching scale [15]. Similar results were obtained more recently in [16] for W -boson plus jet production, where in addition various implementations of the MLM [17] prescription for matching multiparton final states to parton showers have been compared to the methods discussed above. Here, we perform a similar study of systematic uncertainties by comparing the invariant-mass and transverse-momentum distributions as predicted with our implementation of Z' -bosons in MC@NLO with the PYTHIA parton-shower and matrix-element corrections. We also confront these MC predictions with a new computation of Z' -boson production in the framework of joint resummation [18]. In addition, we compare the dependence of the various predictions on the unphysical renormalization and factorization scales as well as on the employed parton densities. The impact of hadronization corrections, dominant electroweak corrections, and non-perturbative effects are also studied.

The remainder of this work is organized as follows: in Sec. II we first describe the PYTHIA framework for Z' -boson production and the associated matching of parton showers with the emission of an additional hard parton. We then discuss our implementation of Z' -boson production in the MC@NLO generator and recall its matching procedure of NLO matrix elements with the HERWIG mechanism of parton showers. We also present briefly our calculation of Z' -boson production using joint resummation. In Sec. III, we define our choice of electroweak SM parameters and define the parameters of our exemplary Z' model. We also discuss the various corrections that we apply to the production cross section, i.e. dominant electroweak corrections, next-to-leading order QCD matrix elements, parton showers, and hadronization. We then compare the numerical impact of these corrections and study the remaining theoretical uncertainties, coming from the choice of renormalization and factorization scales, the parameterization of parton densities, and non-perturbative effects. Our conclusions are given in Sec. IV.

II. THEORETICAL SETUP

In 1984, Green and Schwarz showed that ten-dimensional string theories with $E_8 \times E_8$ or $SO(32)$ gauge symmetry are anomaly-free and thus potentially finite [19]. Among these two gauge groups, only the former contains chiral fermions as they exist in the SM. After compactification, it leads to the E_6 symmetry as an effective GUT group, that can be broken further to [20]

$$E_6 \rightarrow SO(10) \times U(1)_\psi \rightarrow SU(5) \times U(1)_\chi \times U(1)_\psi. \quad (1)$$

While the Z' -bosons corresponding to the additional $U(1)_\psi$ and $U(1)_\chi$ symmetries can in general mix with each other,

$$Z'(\theta) = Z_\psi \cos \theta + Z_\chi \sin \theta \quad \text{and} \quad Z''(\theta) = Z_\psi \sin \theta - Z_\chi \cos \theta, \quad (2)$$

we consider in this work only a TeV-scale Z_χ -boson as an exemplary case, i.e. $\theta = 90^\circ$ in the convention of Ref. [21], and assume the $Z'' \equiv Z_\psi$ to acquire its mass at considerably higher scales, as it is naturally the case in the hierarchy of symmetry breaking of Eq. (1). We will furthermore assume that $SO(10)$ breaks down to $SU(5) \times U(1)_\chi$ at the same scale where $SU(5)$ breaks down to the SM group $SU(3)_C \times SU(2)_L \times U(1)_Y$ with gauge couplings g_s , g , and g' . The $U(1)_\chi$ coupling

$$g_\chi = \sqrt{\frac{5}{3}} g' = \sqrt{\frac{5}{3}} g \tan \theta_W = \sqrt{\frac{5}{3}} \frac{e}{\sqrt{1 - \sin^2 \theta_W}} \quad (3)$$

is then directly related to the coupling g' of the weak hypercharge $U(1)_Y$ by the usual group-theoretical factor $\sqrt{5/3}$. Note that as the $SO(10)$ -breaking scale increases from the $SU(5)$ -breaking scale to the E_6 or Planck scale, g_χ starts

TABLE I: Vector and axial-vector couplings of down- and up-type quarks as well as charged leptons and neutrinos in the E_6 -inspired Z_χ model in the convention of PYTHIA. s_W is the sine of the electroweak mixing angle θ_W .

v_d	a_d	v_u	a_u	v_l	a_l	v_ν	a_ν
$2\sqrt{6}s_W/3$	$-\sqrt{6}s_W/3$	0	$\sqrt{6}s_W/3$	$-2\sqrt{6}s_W/3$	$-\sqrt{6}s_W/3$	$-\sqrt{6}s_W/2$	$-\sqrt{6}s_W/2$

to deviate from $\sqrt{5/3}g'$ to roughly $\sqrt{2/3}$ times this value [22]. Using Eq. (3), we can thus express g_χ in terms of a group-theoretical factor, the $SU(2)_L$ gauge coupling g or alternatively the electromagnetic fine structure constant $\alpha = e^2/(4\pi)$, and the squared sine of the angle θ_W , describing the mixing of the neutral W^0 - and B -bosons to the massless photon and the SM Z -boson of mass m_Z after the breaking of $SU(2)_L \times U(1)_Y$ to $U(1)_{\text{em.}}$. While the photon is protected from further mixing by the exact electromagnetic symmetry, the SM Z -boson can in general mix with the additional Z' -boson with an angle ϕ . Its squared tangent

$$\tan^2 \phi = \frac{m_Z^2 - m_1^2}{m_2^2 - m_Z^2} \quad (4)$$

depends then on the eigenvalues of the $Z - Z'$ mass matrix $m_{1,2}$, which in turn depend on the vacuum expectation values v_{10} and v_{SM} of the $SO(10)$ - and SM-breaking Higgs fields. This mixing can in general induce a coupling of the Z' -boson to the SM W^\pm -bosons, even though they belong to different gauge groups. However, the ratio v_{10}/v_{SM} is usually large and $m_1 \simeq m_Z \ll m_2 \simeq m_{Z'}$, so that $Z - Z'$ mixing will be neglected in the following. The DELPHI collaboration has constrained ϕ to be smaller than a few mrad (1.7 mrad for $m_{Z'} = 440$ GeV in the χ -model) [23].

A. Z' production in PYTHIA

In PYTHIA 6.403 [7], the production of extra neutral gauge bosons in hadron collisions has been implemented including the full interference structure with SM photon and Z -boson exchanges. The Lagrangian describing the interaction of the extra neutral gauge boson Z' with fermions f

$$\mathcal{L} = \frac{g}{4 \cos \theta_W} \bar{f} \gamma^\mu (v_f - a_f \gamma_5) f Z'_\mu \quad (5)$$

has been expressed in terms of generalized vector (v_f) and axial-vector couplings (a_f), which depend in general on the unifying gauge group and the Higgs representations employed to break this group down to the SM gauge group. For the additional $U(1)_\chi$ symmetry, that we use as our standard example, these couplings are given in Tab. I for the down- and up-type quarks as well as for the charged leptons and neutrinos. We will be interested in the Drell-Yan like production of electron-positron pairs

$$q \bar{q} \rightarrow (\gamma, Z, Z') \rightarrow e^- e^+, \quad (6)$$

i.e. the relevant couplings are primarily those of the five light quark flavours $q = u, d, s, c, b$ (with masses m_q much smaller than the partonic centre-of-mass energy \sqrt{s}) and positrons/electrons e^\pm and to a lesser extent those of the other fermions, which contribute to the total decay width appearing in the Z' propagator.

B. Matching of parton showers with LO matrix elements in PYTHIA

The only part of the Drell-Yan like process in Eq. (6) that is sensitive to QCD corrections is the quark-antiquark (and beyond the LO the quark-gluon) initial state. It can give rise to an initial-state parton shower, that is modeled in PYTHIA by starting with the hard scattering partons and then successively reconstructing the preceding branchings in a falling sequence of spacelike virtualities Q^2 . They range from a maximal value $Q_{\text{max}} = m_{Z^{(\prime)}}$, that is of the order of the hard scattering scale, to a cut-off scale $Q_0 = 1$ GeV, that is close to a typical hadron mass.

The scale Q_{max} is, however, not uniquely defined. It can in particular be increased to the hadronic centre-of-mass energy \sqrt{S} , so that the parton shower (PS) populates the full phase space. However, it must then be matched to the QCD matrix element (ME) describing the emission of one extra hard parton

$$q \bar{q} \rightarrow (\gamma, Z, Z') g \quad (7)$$

at $\mathcal{O}(\alpha\alpha_s)$. The emission rate for the final (and normally hardest) $q \rightarrow qg$ emission must therefore be corrected by a factor [9]

$$R_{q\bar{q} \rightarrow (\gamma, Z, Z') g}(s, t) = \frac{(\mathrm{d}\sigma/\mathrm{d}t)_{\mathrm{ME}}}{(\mathrm{d}\sigma/\mathrm{d}t)_{\mathrm{PS}}} = \frac{\sum_{i=\gamma, Z, Z'} [t^2 + u^2 + 2m_i^2 s] + \text{interference terms}}{\sum_{i=\gamma, Z, Z'} [s^2 + m_i^4] + \text{interference terms}}, \quad (8)$$

which always lies between one-half and one. Here, s , t and u refer to the usual Mandelstam variables of the process in Eq. (7), and $m_\gamma = 0$. At the same order, the crossed process

$$qg \rightarrow (\gamma, Z, Z') q \quad (9)$$

can occur, in which case the correction factor is

$$R_{qg \rightarrow \nu q}(s, t) = \frac{(\mathrm{d}\sigma/\mathrm{d}t)_{\mathrm{ME}}}{(\mathrm{d}\sigma/\mathrm{d}t)_{\mathrm{PS}}} = \frac{\sum_{i=\gamma, Z, Z'} [s^2 + u^2 + 2m_i^2 t] + \text{interference terms}}{\sum_{i=\gamma, Z, Z'} [(s - m_i^2)^2 + m_i^4] + \text{interference terms}}. \quad (10)$$

Since this factor always lies between one and three, the $g \rightarrow q\bar{q}$ splitting must be preweighted by a factor three in order to correctly reproduce the s -channel graph $qg \rightarrow q^* \rightarrow (\gamma, Z, Z') q$. Besides the dominant QCD radiation, we will also briefly investigate the effect of the relatively suppressed QED radiation (e.g. $q \rightarrow q\gamma$) as well as the corrections induced by the hadronization of the additional partons.

In addition to the transverse momentum p_T generated by hard emission and/or the initial-state parton shower, an average intrinsic transverse-momentum $\langle k_T \rangle$ can be assigned to the shower initiator in order to take into account the transverse motion of quarks inside the original hadron. As the shower does not evolve below $Q_0 = 1$ GeV, this same value is retained in PYTHIA as the default value for $\langle k_T \rangle$. However, just like Q_{\max} , $Q_0 \equiv \langle k_T \rangle$ is not uniquely defined and furthermore closely related to the non-perturbative regime of QCD. We therefore set $\langle k_T \rangle = 0$ in the following.

PYTHIA allows in principle also for the participation of multiple parton pairs in hadronic collisions. We do, however, not make use of this possibility, as it has little numerical effect and its description in perturbative QCD remains controversial.

C. Implementation of Z' -bosons in MC@NLO

In MC@NLO [11], the implementation of SM Z -boson interactions with fermions f is based on the Lagrangian [24]

$$\frac{g}{\cos\theta_W} \bar{f} \gamma^\mu (a_f + b_f \gamma_5) f Z_\mu. \quad (11)$$

For photon interactions, $a_f = e_f \sin\theta_W \cos\theta_W$, where e_f is the fractional fermion charge, and $b_f = 0$. The vector coupling a_f and the axial vector coupling b_f are related to those defined in PYTHIA (see Eq. (5)) by $a_f \rightarrow v_f/4$ and $b_f \rightarrow -a_f/4$. They are combined to form the coefficients $A_f = a_f^2 + b_f^2$ and $B_f = 2a_f b_f$, that appear in the squared matrix elements

$$\begin{aligned} |\overline{\mathcal{M}_i}|^2(q\bar{q} \text{ or } qg \rightarrow \gamma, Z \rightarrow e^- e^+ + X) &= \frac{1}{4} e^4 C_i \left\{ \frac{e_q^2}{M^4} T_i^{1,0}|_{1,0} \right. \\ &+ \frac{1}{\sin^4\theta_W \cos^4\theta_W} \frac{1}{(M^2 - m_Z^2)^2 + (\Gamma_Z m_Z)^2} T_i^{A_l, B_l}|_{A_q, B_q} \\ &\left. - \frac{2e_q}{M^2 \sin^2\theta_W \cos^2\theta_W} \frac{M^2 - m_Z^2}{(M^2 - m_Z^2)^2 + (\Gamma_Z m_Z)^2} T_i^{a_l, b_l}|_{a_q, b_q} \right\}, \quad (12) \end{aligned}$$

that have been averaged/summed over initial/final spins and colours. For the LO Drell-Yan (DY) process in Eq. (6), the colour factor is $C_{\mathrm{DY}} = N_C/N_C^2 = 1/3$ and

$$T_{\mathrm{DY}}|_{A_q, B_q}^{A_l, B_l} = 8 [A_l A_q (t_{\mathrm{DY}}^2 + u_{\mathrm{DY}}^2) - B_l B_q (t_{\mathrm{DY}}^2 - u_{\mathrm{DY}}^2)], \quad (13)$$

where $M^2 = s_{\mathrm{DY}}$ is the invariant mass of the lepton pair and s_{DY} , t_{DY} , and u_{DY} refer to the Mandelstam variables of the DY-process in Eq. (6). The NLO QCD-corrections to the DY-process have been implemented in MC@NLO using the same convention [24].

One major new and technical aspect of our work is the implementation of Z' -boson interactions and exchanges in the framework described above. To this end, we have defined the mass and width of the Z' -boson as well as its couplings in the convention of PYTHIA. The squared matrix element has also been modified,

$$\begin{aligned}
|\overline{\mathcal{M}_i}|^2(q\bar{q} \text{ or } qg \rightarrow \gamma, Z, Z' \rightarrow e^- e^+ + X) = & \frac{1}{4} e^4 C_i \left\{ \frac{e_q^2}{M^4} T_i|_{1,0}^{1,0} \right. \\
& + \frac{1}{\sin^4 \theta_W \cos^4 \theta_W} \frac{1}{(M^2 - m_Z^2)^2 + (\Gamma_Z m_Z)^2} T_i|_{A_q, B_q}^{A_l, B_l} \\
& + \frac{1}{\sin^4 \theta_W \cos^4 \theta_W} \frac{1}{(M^2 - m_{Z'}^2)^2 + (\Gamma_{Z'} m_{Z'})^2} T_i|_{A'_q, B'_q}^{A'_l, B'_l} \\
& - \frac{2e_q}{M^2} \frac{1}{\sin^2 \theta_W \cos^2 \theta_W} \frac{M^2 - m_Z^2}{(M^2 - m_Z^2)^2 + (\Gamma_Z m_Z)^2} T_i|_{a_q, b_q}^{a_l, b_l} \\
& - \frac{2e_q}{M^2} \frac{1}{\sin^2 \theta_W \cos^2 \theta_W} \frac{M^2 - m_{Z'}^2}{(M^2 - m_{Z'}^2)^2 + (\Gamma_{Z'} m_{Z'})^2} T_i|_{a'_q, b'_q}^{a'_l, b'_l} \\
& + 2 \frac{1}{\sin^4 \theta_W \cos^4 \theta_W} \frac{(M^2 - m_Z^2)(M^2 - m_{Z'}^2) + \Gamma_Z m_Z \Gamma_{Z'} m_{Z'}}{[(M^2 - m_Z^2)^2 + (\Gamma_Z m_Z)^2] \times [(M^2 - m_{Z'}^2)^2 + (\Gamma_{Z'} m_{Z'})^2]} \\
& \times \left. T_i|_{a_q a'_q + b_q b'_q, a_q b'_q + a'_q b_q}^{a_l a'_l + b_l b'_l, a_l b'_l + a'_l b_l} \right\}. \tag{14}
\end{aligned}$$

It includes now the squared Z' -boson exchange as well as its interferences with the photon and SM Z -boson exchanges. Note that it is not sufficient to change only the Z -boson mass in the existing MC@NLO implementation, but that it is also necessary to change the Z -boson width as well as the couplings. As a consequence, all observables change: the mass spectrum due to the modified width, the forward-backward asymmetries due to the modified couplings, etc. Furthermore, even if one changes all of these parameters, one still has $\gamma - Z'$ interference, but no $Z - Z'$ interference. We have checked numerically that these modifications induce large differences already in the total cross section.

D. Matching of parton showers with NLO matrix elements in MC@NLO

In HERWIG [12], parton showers are generated by a coherent branching algorithm with parton splittings $i \rightarrow jk$, whose energy fractions $z_j = E_j/E_i$ are distributed according to the LO DGLAP splitting functions. Phase space is restricted to an angular ordered region, which automatically takes infrared singularities into account, i.e. at each branching, the angle between the two emitted partons is smaller than that of the previous branching. The emission angles $\xi_{jk} = (p_j \cdot p_k)/(E_j E_k) \simeq \frac{1}{2} \theta_{jk}^2$ are distributed according to Sudakov form factors, that sum virtual corrections and unresolved real emissions and normalize the branching distributions to give the probabilistic interpretation needed for a MC simulation. For initial-state radiation, the parton shower follows, of course, a backward evolution. It is terminated when $\xi_{jk} < Q_0^2/E_i^2$, where the space-like cut-off scale Q_0 is set to 2.5 GeV by default. Below this scale, a non-perturbative stage is imposed. In particular, a splitting of non-valence partons is enforced to allow for a smooth transition to the valence partons inside the outer hadron. Although HERWIG also allows for the simulation of a soft underlying event, we have not made use of this possibility. Since the parton shower is supposed to describe only the soft/collinear region, any initial-state emission outside this region, i.e. where $\xi > z^2$, is suppressed.

As was the case for PYTHIA, hard matrix element corrections for SM vector boson production have been implemented in HERWIG [13], where radiation in the region $\xi > z^2$ can now be allowed. It is then distributed according to the matrix element describing the emission of an additional parton. In the soft region $\xi < z^2$ already populated by the parton shower, the emission of the hardest (largest p_T) parton generated so far is reweighted in order to avoid double counting. Note that this need not be the first emission, since angular ordering does not necessarily imply ordering in transverse momentum. Note also that the normalization of the total cross section is still accurate to LO only.

A NLO accuracy of the total cross section has been achieved in MC@NLO [11] through an implementation of NLO cross sections, matched to the HERWIG parton shower. Instead of the LO matrix element implemented in the standard version of HERWIG, two separate samples of Born-like or standard (S) and hard emission (H) events are generated, that can have weight $w_i^{(S,H)} = \pm 1$ and are statistically distributed according to the positive-definite standard and hard contributions to the NLO cross section $J_{S,H}$. These are made separately finite by adding and subtracting the NLO part of the expanded Sudakov form factor and are explicitly defined in Ref. [11]. The total cross section is then given by $\sigma_{\text{tot}} = \sum_{i=1}^{N_{\text{tot}}} w_i^{(S,H)} (J_H + J_S)/N_{\text{tot}}$.

E. Joint transverse-momentum and threshold resummation for Z' -bosons

The LO matrix element predictions for Z' -production are affected by fixed order (F.O.) QCD corrections, that are logarithmically enhanced, when the Z' -boson is produced close to the partonic threshold, i.e. $z = M^2/s \rightarrow 1$, or when its transverse momentum is small, i.e. $p_T \rightarrow 0$. These corrections must then be resummed (res) to all orders, which is most easily achieved in Mellin (N) and impact parameter (b) space, and matched to the F.O. prediction by subtracting from their sum the perturbatively expanded (exp) resummed prediction, i.e.

$$\frac{d^2\sigma}{dM^2 dp_T^2} = \frac{d^2\sigma^{(\text{F.O.})}}{dM^2 dp_T^2} + \oint_C \frac{dN}{2\pi i} \tau^{-N} \int_0^\infty \frac{b db}{2} J_0(b p_T) \left[\frac{d^2\sigma^{(\text{res})}}{dM^2 dp_T^2}(N, b) - \frac{d^2\sigma^{(\text{exp})}}{dM^2 dp_T^2}(N, b) \right]. \quad (15)$$

In this way, a uniform precision is obtained, and the large theoretical (renormalization and factorization scale) uncertainties are reduced. The NLO cross section for Drell-Yan processes (with $\tau = M^2/S$)

$$\frac{d^2\sigma^{(\text{F.O.})}}{dM^2 dp_T^2} = \sum_{a,b} \int_\tau^1 dx_a \int_{\tau/x_a}^1 dx_b f_{a/h_a}(x_a; \mu_F) f_{b/h_b}(x_b; \mu_F) \left[\delta(p_T^2) \delta(1-z) \hat{\sigma}_{ab}^{(0)} + \frac{\alpha_s(\mu_R)}{\pi} \hat{\sigma}_{ab}^{(1)}(z) + \mathcal{O}(\alpha_s^2) \right] \quad (16)$$

is well-known [24], and the necessary modifications for implementing Z' -bosons in the $\mathcal{O}(\alpha_s^i)$ partonic cross sections

$$\hat{\sigma}_{ab}^{(i)} = \frac{1}{2s} \overline{|\mathcal{M}_i|^2} \frac{dt}{8\pi s} \quad (17)$$

have already been discussed above.

Since the p_T - [25] and threshold-enhanced contributions [26] are both due to soft-gluon emission in the initial state, they may be resummed at the same time [18, 27, 28]. The logarithms are then organized by the function

$$\chi(\bar{b}, \bar{N}) = \bar{b} + \frac{\bar{N}}{1 + \eta \bar{b}/\bar{N}} \quad \text{with} \quad \bar{b} \equiv b M e^{\gamma_E}/2 \quad \text{and} \quad \bar{N} \equiv N e^{\gamma_E}, \quad (18)$$

whose form with $\eta = 1/4$ is constrained by the requirement that the leading and next-to-leading logarithms in \bar{b} and \bar{N} are correctly reproduced in the limits $\bar{b} \rightarrow \infty$ and $\bar{N} \rightarrow \infty$, respectively. The choice of Eq. (18) with $\eta = 1/4$ avoids the introduction of sizeable subleading terms into perturbative expansions of the resummed cross section at a given order in α_s , which are not present in fixed-order calculations [29]. The resummed cross section

$$\begin{aligned} \frac{d^2\sigma^{(\text{res})}}{dM^2 dp_T^2}(N, b) &= \sum_{a,b,c} f_{a/h_a}(N+1; \mu_F) f_{b/h_b}(N+1; \mu_F) \hat{\sigma}_{c\bar{c}}^{(0)} \exp[\mathcal{G}_c(N, b; \alpha_s, \mu_R)] \\ &\times \left[\delta_{ca} \delta_{c\bar{b}} + \sum_{n=1}^{\infty} \left(\frac{\alpha_s(\mu_R)}{\pi} \right)^n \mathcal{H}_{ab \rightarrow c\bar{c}}^{(n)}(N; \mu_R, \mu_F) \right] \end{aligned} \quad (19)$$

can then be factorized into a regular part with

$$\mathcal{H}_{ab \rightarrow c\bar{c}}^{(1)}(N; \mu_R, \mu_F) = \delta_{ca} \delta_{c\bar{b}} H_{c\bar{c}}^{(1)}(\mu_R) + \delta_{ca} C_{c/b}^{(1)}(N) + \delta_{c\bar{b}} C_{c/a}^{(1)}(N) + \left(\delta_{ca} \gamma_{c/b}^{(1)}(N) + \delta_{c\bar{b}} \gamma_{c/a}^{(1)}(N) \right) \ln \frac{M^2}{\mu_F^2}, \quad (20)$$

where in the Drell-Yan resummation scheme

$$H_{c\bar{c}}^{(1)}(\mu_R) \equiv 0, \quad C_{q/q}^{(1)}(N) = \frac{2}{3N(N+1)} + \frac{\pi^2 - 8}{3}, \quad \text{and} \quad C_{q/g}^{(1)}(N) = \frac{1}{2(N+1)(N+2)}, \quad (21)$$

and a perturbatively calculable eikonal factor

$$\mathcal{G}_c(N, b; \alpha_s, \mu_R) = g_c^{(1)}(\lambda) \ln \chi + g_c^{(2)}(\lambda; \mu_R), \quad (22)$$

which depends through the functions

$$g_c^{(1)}(\lambda) = \frac{A_c^{(1)}}{\beta_0} \frac{2\lambda + \ln(1-2\lambda)}{\lambda} \quad \text{and} \quad (23)$$

$$\begin{aligned} g_c^{(2)}(\lambda; \mu_R) &= \frac{A_c^{(1)} \beta_1}{\beta_0^3} \left[\frac{1}{2} \ln^2(1-2\lambda) + \frac{2\lambda + \ln(1-2\lambda)}{1-2\lambda} \right] \\ &+ \left[\frac{A_c^{(1)}}{\beta_0} \ln \frac{M^2}{\mu_R^2} - \frac{A_c^{(2)}}{\beta_0^2} \right] \left[\frac{2\lambda}{1-2\lambda} + \ln(1-2\lambda) \right] + \frac{B_c^{(1)}(N)}{\beta_0} \ln(1-2\lambda) \end{aligned} \quad (24)$$

on the logarithm $\lambda = \beta_0/\pi \alpha_s(\mu_R) \ln \chi$. The anomalous dimensions $\gamma_{c/a}^{(1)}(N)$ are the N -moments of the $\mathcal{O}(\alpha_s)$ Altarelli-Parisi splitting functions. Up to next-to-leading logarithmic order, the coefficients needed in $g_c^{(1,2)}$ are

$$A_q^{(1)} = C_F, \quad A_q^{(2)} = C_F \left[C_A \left(\frac{67}{36} - \frac{\pi^2}{12} \right) - \frac{5}{9} T_R N_f \right], \quad \text{and} \quad B_q^{(1)}(N) = -\frac{3}{2} C_F + 2\gamma_{q/q}^{(1)}(N). \quad (25)$$

The usual coefficients of the QCD β -function are

$$\beta_0 = \frac{1}{12}(11 C_A - 4 T_R N_f) \quad \text{and} \quad \beta_1 = \frac{1}{24}(17 C_A^2 - 10 T_R C_A N_f - 6 C_F T_R N_f), \quad (26)$$

the number of effectively massless quark flavours is N_f , and $C_F = 4/3$, $C_A = 3$, and $T_R = 1/2$ are the usual QCD colour factors. Re-expanding the resummed cross section leads to

$$\begin{aligned} \frac{d^2 \sigma^{(\text{exp})}}{dM^2 dp_T^2}(N, b) &= \sum_{a,b,c} f_{a/h_a}(N+1; \mu_F) f_{b/h_b}(N+1; \mu_F) \hat{\sigma}_{c\bar{c}}^{(0)} \\ &\times \left[\delta_{ca} \delta_{\bar{c}b} + \sum_{n=1}^{\infty} \left(\frac{\alpha_s(\mu_R)}{\pi} \right)^n \left(\Sigma_{ab \rightarrow c\bar{c}}^{(n)}(N, b) + \mathcal{H}_{ab \rightarrow c\bar{c}}^{(n)}(N; \mu_R, \mu_F) \right) \right] \end{aligned} \quad (27)$$

with the coefficient

$$\Sigma_{ab \rightarrow c\bar{c}}^{(1)}(N, b) = -2 \left[A_c^{(1)} \delta_{ca} \delta_{\bar{c}b} \ln^2 \chi + \left(B_c^{(1)} \delta_{ca} \delta_{\bar{c}b} + \delta_{ca} \gamma_{\bar{c}/b}^{(1)}(N) + \delta_{\bar{c}b} \gamma_{c/a}^{(1)}(N) \right) \ln \chi \right], \quad (28)$$

which matches precisely with the NLO cross section.

III. NUMERICAL COMPARISON

In this section, we compare the three different theoretical approaches to Z' -boson production at the LHC discussed above, i.e. the matching of LO matrix elements with parton showers as implemented in PYTHIA, the matching of NLO matrix elements with parton showers in our modified version of MC@NLO, and the matching of NLO matrix elements with our improved formalism of joint resummation at next-to-leading logarithmic (NLL) order. For a comparison of joint resummation with transverse-momentum and threshold resummation in Drell-Yan like processes we refer the reader to Ref. [18].

We first fix our choice of parton densities and of the strong, electroweak, and extra gauge-boson parameters and demonstrate that the three theoretical predictions coincide at the LO partonic level for both the mass- and the p_T -spectrum. Next, we show the impact of the dominant electroweak corrections by running the fixed electromagnetic coupling from zero momentum transfer to the mass of the Z' -boson. We then analyze separately the different levels of improvement made possible in the three theoretical approaches, before comparing the three “best versions” directly with each other. Finally, we discuss the impact of the remaining theoretical uncertainties, coming from variations of the renormalization and factorization scales and the parton densities, on the theoretical predictions.

A. Choice of strong, electroweak, and extra gauge-boson parameters

We will make predictions for pp collisions at the LHC at a centre-of-mass energy of $\sqrt{S} = 14$ TeV, choosing the CTEQ6L (LO) and CTEQ6M (NLO $\overline{\text{MS}}$) [30] sets as our default for the parton densities in the protons for LO and NLO/NLL calculations, respectively. The strong coupling constant $\alpha_s(\mu_R)$ is always computed with two-loop accuracy, $\Lambda_{\overline{\text{MS}}}^{n_f=5} = 226$ MeV, and identifying the renormalization scale μ_R (as well as the factorization scale μ_F) with the invariant mass of the lepton pair M . As is customary, the theoretical uncertainty is estimated by varying the scales by a factor of two around the central value.

For the electroweak mass, width, and coupling parameters, we use the values of the 2002 Review of the Particle Data Group [31], i.e. $m_Z = 91.188$ GeV, $\Gamma_Z = 2.4952$ GeV, $\alpha = 1/137.04$, and $\sin^2 \theta_W = 0.23113$, which are (still) used as default in the Z' analysis of the ATLAS collaboration. The only value that has changed in 2006 is $\sin^2 \theta_W = 0.23122$ [32], but the numerical impact of this change remains visibly small. Using these parameters, a Z' -boson mass of 1 TeV, running the fine-structure constant to $\alpha(1 \text{ TeV}) = 1/124.43$, and including the NLO QCD correction factor $1 + \alpha_s(\mu_R)/\pi$ for Z' -decays into quarks, we compute the total width of the Z' -boson in the χ -model within PYTHIA

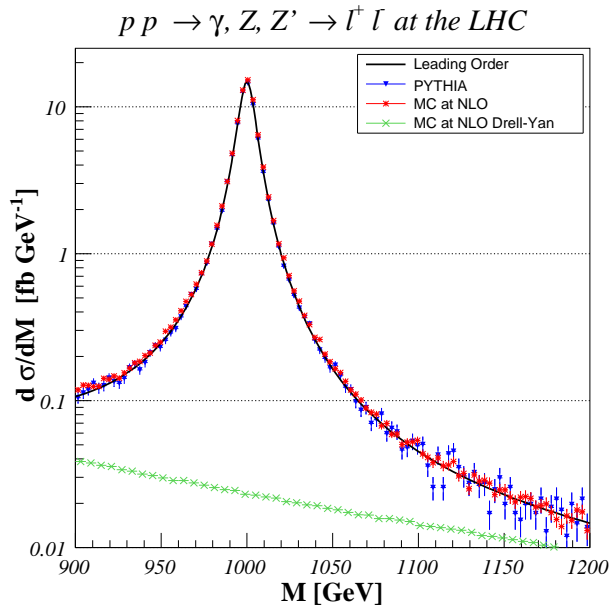


FIG. 1: The LO mass-spectrum for Z' production with fixed α in PYTHIA (triangles), MC@NLO (stars) and at parton level (full line and circle), compared to the SM Drell-Yan background in MC@NLO (crosses).

(see Sec. II A) to be $\Gamma = 12.04$ GeV. Its branching ratio to electron-positron pairs, representing the signal, is found to be 5.98%. These values are then passed as parameters to our modified MC@NLO and new resummation programs.

In order to set a common theoretical basis, we show in Fig. 1 the invariant mass-spectrum of the electron-positron pair in LO QCD, i.e. without any parton shower, matrix element correction, resummation, or hadronization effects. The PYTHIA (triangles), MC@NLO (stars), and parton level (full line) mass spectra, shown in the mass range of 900 to 1200 GeV around the mass peak of the Z' -boson at 1 TeV, coincide perfectly. For comparison, we also show the differential cross section for the SM Drell-Yan process in MC@NLO (crosses), which coincides with the corresponding LO and PYTHIA predictions and represents the dominant (irreducible) background to the Z' -boson signal. Far from the resonance region, the two mass spectra would, of course, coincide. The transverse momentum of the lepton pair (p_T) is exactly zero in PYTHIA and at parton level, while the forced splitting of non-valence partons in MC@NLO induces a distribution that extends to non-zero values of p_T even when the parton shower is switched off. Since this distribution is unphysical, we do not show it here. When integrated over p_T , the MC@NLO total cross section coincides, however, with PYTHIA's and the one at parton level.

The dominant electroweak corrections can be resummed by running the fixed value of the fine-structure constant $\alpha = 1/137.04$ in Fig. 1 to the value $\alpha = 1/124.43$ at the mass of the Z' -boson in the $\overline{\text{MS}}$ -scheme. The ratio $\alpha^2(M)/\alpha^2(0)$ then induces an increase of about 22% in the cross sections shown in Fig. 1. In the following, we will always use a running value of α .

B. Numerical results with PYTHIA

In Fig. 2, we show the three different ways of improving on the parton-level predictions that are implemented in PYTHIA, where one can either add QCD parton showers in the soft and collinear regions (circles), corresponding to the leading-logarithmic (LL) approximation, or in the full phase space (triangles), which however overestimates the cross section, so that it must be renormalized to the matrix element describing the emission of an additional hard parton (squares). By definition, neither the total cross section nor the mass spectrum are changed and remain accurate to LO only, as can be seen from the fact that all histograms on the left-hand side of Fig. 2 coincide, after normalization to the LO prediction and within the statistical error bars, with unity. The right-hand side of Fig. 2 demonstrates that the zero transverse momentum of the Z' -boson is smeared by the parton showers. It then peaks around 3 GeV and extends up to 700 GeV (see insert) and even beyond, if the available phase space is opened to the full hadronic centre-of-mass energy as proposed by the “power shower” prescription. Note that strictly speaking the LL approximation is, of course, no longer valid there. Normalizing the “power shower” to the correct QCD matrix element describing one real emission brings the integrated cross section back into agreement with the LO prediction,

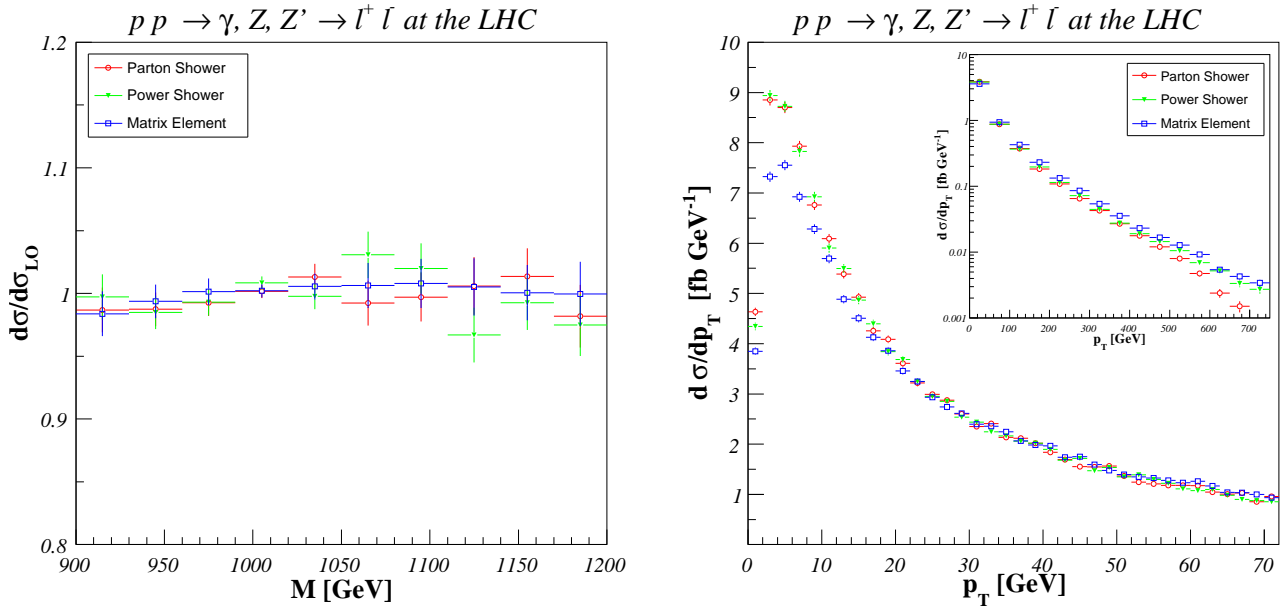


FIG. 2: Mass (left) and transverse-momentum spectra (right) with PYTHIA with soft/collinear QCD parton showers (circles), QCD parton showers populating the full phase space (triangles), and after adding LO matrix element corrections (squares). The mass spectra have been normalized to the LO QCD prediction.

as the increase of the cross section at large p_T is compensated by a reduction at small p_T . These predictions may be improved further in PYTHIA by adding QED parton showers, which are, however, formally suppressed by a factor of α/α_s , so that their influence would not be visible in Fig. 2. The emitted additional partons may furthermore hadronize, which is modeled in PYTHIA with the Lund string model, but we have checked again that the shapes of the distributions in Fig. 2 would not change significantly.

C. Numerical results with MC@NLO

With MC@NLO it is possible to correct not only the transverse-momentum shape, but also the normalization of the total cross section. In our implementation, this is now also possible for Z' production at the LHC. This is demonstrated in Fig. 3, where we show on the left-hand side that the NLO correction factor

$$K \equiv \frac{d\sigma_{\text{NLO}}}{d\sigma_{\text{LO}}} \simeq 1.26 \quad (29)$$

at the resonance ($M = 1$ TeV) is quite significant and depends also slightly on the invariant mass of the lepton pair. By definition, the normalization remains again unchanged by the HERWIG parton shower, which affects, however, strongly the p_T -spectrum (right). While the fixed-order prediction diverges as $p_T \rightarrow 0$, its logarithmic singularity is effectively resummed by the parton shower and leads to a smooth turnover with a maximum at around 8 GeV, i.e. at a value that is considerably larger than in the case of PYTHIA. Note that the parton shower in MC@NLO replaces part of the NLO contribution, so that switching it off (not shown) does not lead to a fully correct NLO prediction. As was already the case in PYTHIA, we have checked that adding QED parton showers or hadronization, which is modeled in HERWIG with the cluster model, does not lead to visible changes in the distributions of Fig. 3.

D. Numerical results with joint resummation

Theoretically, the most precise predictions are obtained if logarithmically enhanced soft and collinear parton emission is analytically resummed, both close to threshold and close to $p_T \simeq 0$, as described in Sec. II E above. As can be seen from Fig. 4 (left), the NLO K -factor (dashed) is increased further by the resummed contributions, in particular in pure threshold resummation (dotted), which is only approximately described by joint resummation, as

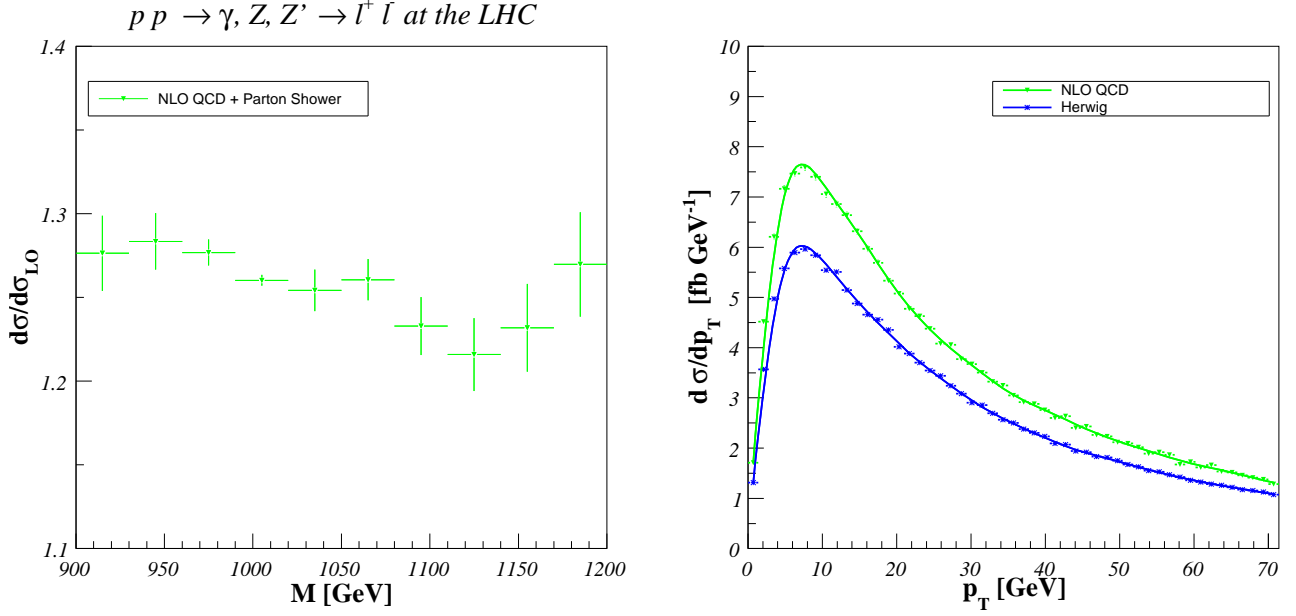


FIG. 3: Mass (left) and transverse-momentum spectra (right) after matching the NLO QCD corrections to the HERWIG QCD parton shower (triangles). The mass spectra have been normalized to the LO QCD prediction.

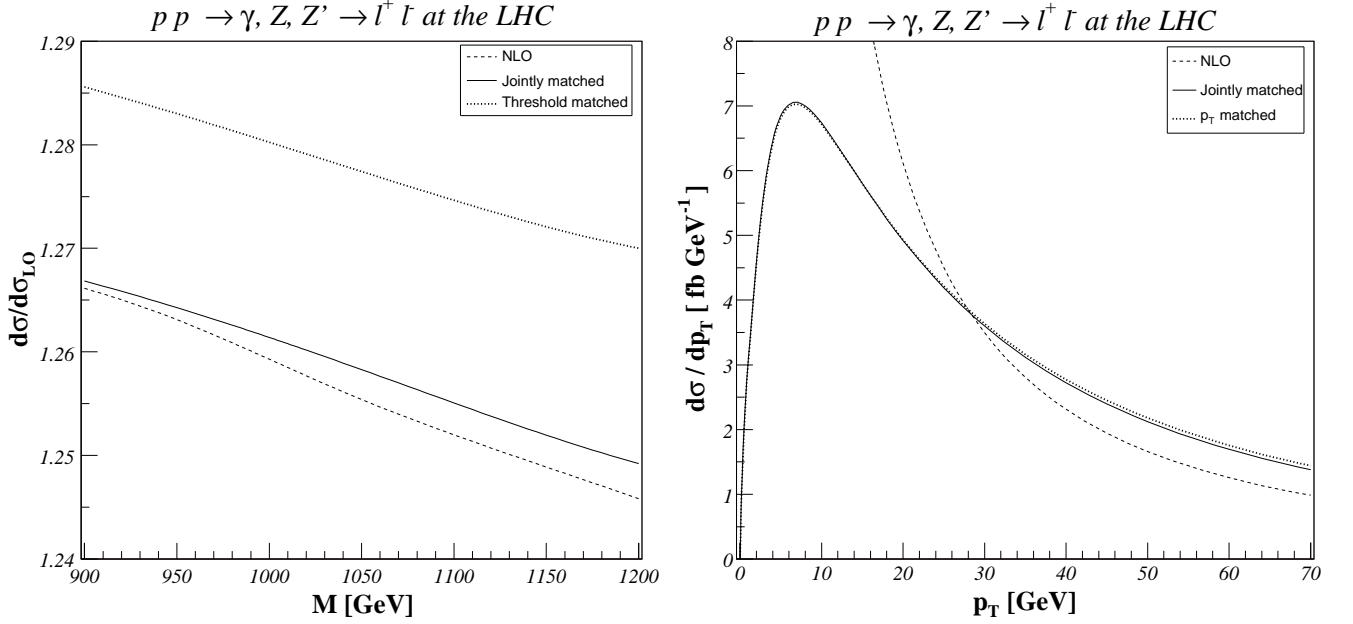


FIG. 4: Mass (left) and transverse-momentum spectra (right) in NLO QCD (dashed) and after resumming threshold and p_T logarithms (dotted) or both at the same time (full line). The resummed cross sections have been matched to those at NLO, and the mass spectra have been normalized to the LO QCD prediction.

we are still relatively far from the production threshold at $\sqrt{S} = 14$ TeV. Only for larger values of M would the joint and threshold resummed predictions coincide. As the additional increase in K is only of the order of a few percent, the prediction is nicely stabilized. We have checked that the K -factors of 1.26 at NLO and 1.28 at NNLO [10] for Drell-Yan lepton pairs with mass 1 TeV coincide precisely with our NLO and threshold resummed results. Fig. 4 (right) demonstrates that the true NLO p_T -distribution (dashed) diverges as $p_T \rightarrow 0$, as it must, and does indeed not exhibit the unphysical maximum of MC@NLO without parton showers around 10 GeV. Resummation leads again to a smooth turnover with a maximum at around 8 GeV. Note that the jointly resummed prediction (full) follows the

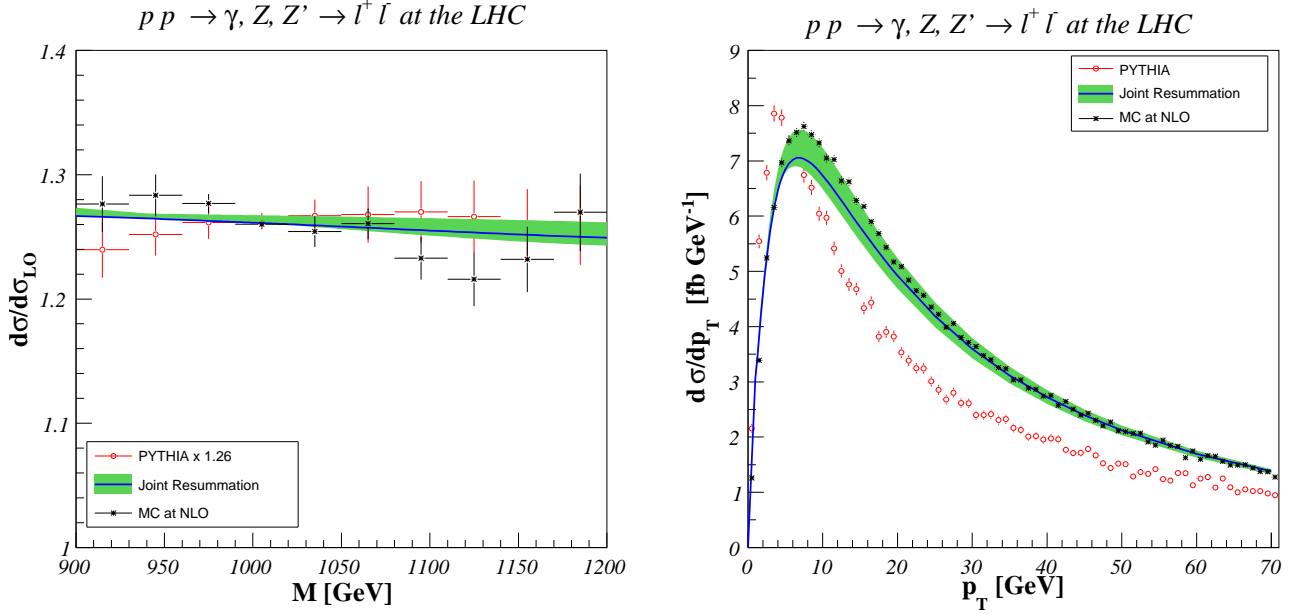


FIG. 5: Mass (left) and transverse-momentum spectra (right) in PYTHIA with LO matrix elements matched to QCD parton showers (circles), in MC@NLO with NLO matrix elements matched to the HERWIG QCD parton shower (stars), and after matching the NLO QCD corrections to joint resummation (full line). The mass spectra have been normalized to the LO QCD prediction, and the renormalization and factorization scale uncertainties in the resummed predictions are indicated as shaded bands.

one with p_T -resummation (dotted) very closely, as is to be expected from the definition of the variable χ and the form of the function \mathcal{G}_c (see above).

E. Comparison of numerical results and theoretical uncertainties

We now confront the “best versions” of the three different theoretical approaches with each other, superimposing in Fig. 5 the LO matrix element corrected predictions obtained with PYTHIA’s “power shower” (circles), the NLO matrix element corrected predictions obtained with MC@NLO’s parton shower (stars), and the jointly resummed prediction matched to the NLO matrix elements (full line). The correction factors for the mass spectra (left), which have been normalized to the LO QCD prediction, show only a very weak mass dependence. We have multiplied the PYTHIA mass spectrum by hand with a global K -factor of 1.26. Otherwise, within the statistical error bars the PYTHIA K -factor would just be unity, since the normalization of the total cross section is changed neither by the parton shower nor by the LO matrix element correction, that serves to bring the “power shower” back into agreement with the LO QCD prediction. The MC@NLO K -factor agrees almost perfectly with the one of joint resummation, since we saw in Fig. 4 (left) that threshold and joint resummation lead only to a very modest increase of the NLO K -factor. The theoretical uncertainty induced in the resummed prediction through the simultaneous variation of the renormalization and factorization scale by a factor of two around the central scale M is also considerably smaller than the K -factor, indicating a nice stabilization of the theoretical prediction. The p_T -spectra (right) are, for all three improvements, no longer divergent. The PYTHIA prediction rises and falls rather steeply around its maximum at 3 GeV, whereas the MC@NLO and resummed predictions rise and fall more slowly around the peak at 8 GeV, which has furthermore a slightly smaller cross section. The agreement between MC@NLO and joint resummation is impressive, in particular for a scale choice of $M/2$ (upper end of the shaded band) at low p_T and M at intermediate p_T . We can therefore conclude that our implementation of Z' production in MC@NLO reaches almost the same level of precision as our joint resummation calculation, but offers the additional advantage of an easy implementation in the analysis chains of the LHC experiments.

The scale uncertainty of the total cross section (integrated over all transverse momenta and over the invariant mass in the range from 900 to 1200 GeV) is shown in Fig. 6. The LO QCD prediction (full) agrees with the PYTHIA prediction (dot-dashed) at the same order, as the total cross section and its scale dependence is not modified by the parton shower. Since $\alpha_s(\mu_R)$ does not enter the calculation at this order, the full scale dependence is in fact due to

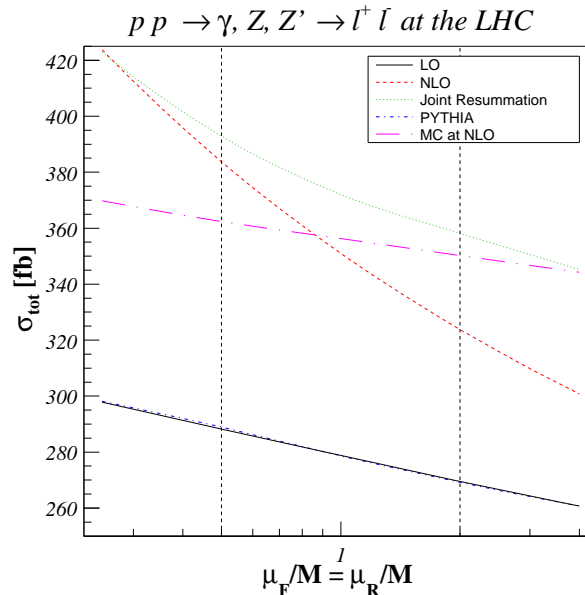


FIG. 6: Dependence of the total Z' -boson production cross section at the LHC on the common factorization/renormalization scale $\mu_{F,R}$ in LO QCD (full), NLO QCD (dashed), and after matching the NLO QCD corrections to joint resummation (dotted), LO matrix elements to the PYTHIA parton shower (dot-dashed), and NLO matrix elements to the HERWIG parton shower (long dot-dashed).

the factorization scale. The LO scale dependence does, however, not give a reliable estimate of the theoretical error, since the NLO cross section (dashed) is considerably larger. At NLO, the factorization scale dependence is reduced as expected, but $\alpha_s(\mu_R)$ makes its appearance, so that an additional renormalization scale dependence is introduced. The total NLO scale dependence is reduced to 9% (vertical lines), once the leading and next-to-leading logarithms (NLL) are resummed (dotted). The MC@NLO prediction (long dot-dashed) agrees with the one at NLO (dashed) for the central scale, but has a weaker scale dependence due to the resummation of leading logarithms in the parton shower [33]. Since both the type (p_T vs. joint) and order (LL vs. NLL) of the resummed logarithms differ between MC@NLO and joint resummation, the two scale variations need not (and do not) coincide.

We estimate in Fig. 7 the theoretical uncertainty coming from different parameterizations of parton densities. Since the invariant mass M of the lepton pair is correlated with the momentum fractions $x_{a,b}$ of the partons in the external protons, the normalized mass spectra (left) are indicative of the different shapes of the quark and gluon densities in the CTEQ6M (full) and MRST 2004 NLO [34] (dashed) parameterizations. The latter also influence the transverse-momentum spectra, which are slightly harder for MRST 2004 NLO than for CTEQ6M. The shaded bands show the uncertainty induced by variations along the 20 independent directions that span the 90% confidence level of the data sets entering the CTEQ6 global fit [36]. It remains modest, i.e. about 8%, and is thus slightly smaller than the scale uncertainty of 9%.

The uncertainty at low transverse momenta coming from non-perturbative effects in the PDFs is usually parameterized with a Gaussian form factor describing the intrinsic transverse momentum of partons in the proton. We show in Fig. 8 the effects coming from three different choices of the form factor, i.e. those of Ladinsky-Yuan (LY-G) [37], Brock-Landry-Nadolsky-Yuan (BLNY) [38], and Konychev-Nadolsky (KN) [39], on the quantity

$$\Delta = \frac{d\sigma^{(\text{res.}+\text{NP})}(\mu_R = \mu_F = M) - d\sigma^{(\text{res.})}(\mu_R = \mu_F = M)}{d\sigma^{(\text{res.})}(\mu_R = \mu_F = M)}. \quad (30)$$

It is obvious that these non-perturbative contributions are under good control, as their effect is always less than 5% for $p_T > 5$ GeV and thus considerably smaller than the scale and PDF uncertainties.

IV. CONCLUSIONS

In summary, we have improved the theoretical predictions for the production of extra neutral gauge bosons at hadron colliders by implementing the Z' bosons in the MC@NLO generator and by computing their differential

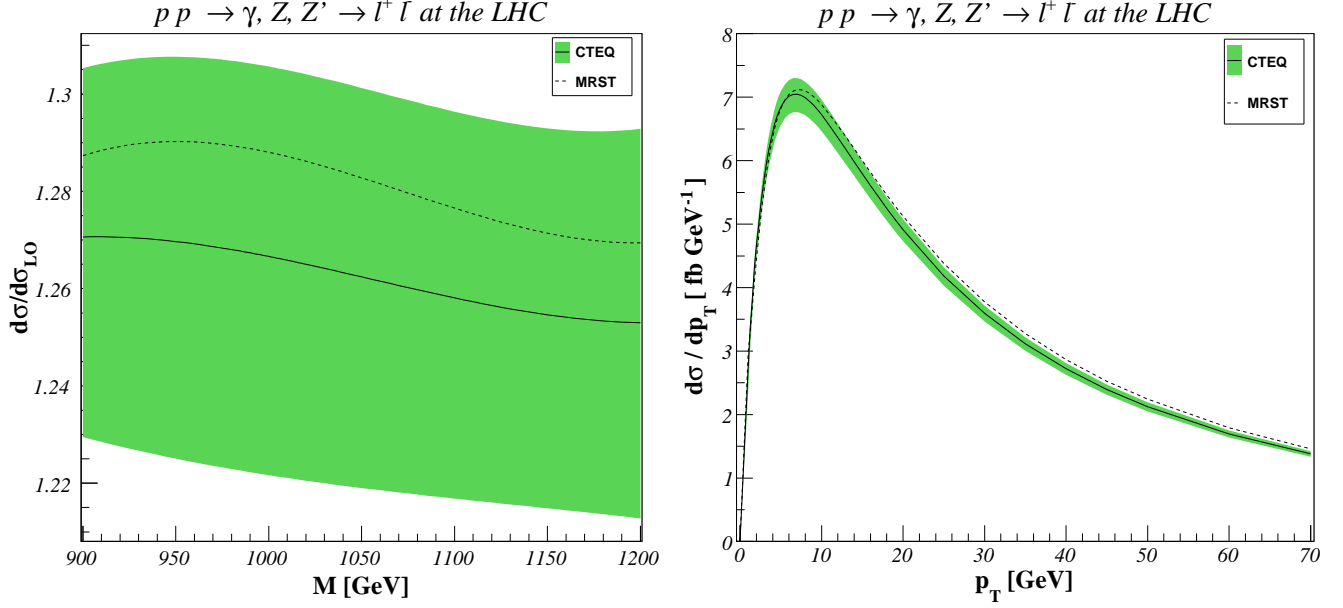


FIG. 7: Mass (left) and transverse-momentum spectra (right) after matching the NLO QCD corrections to joint resummation with CTEQ6M (full) and MRST 2004 NLO [34] (dashed) parton densities. The mass spectra have been normalized to the LO QCD prediction using CTEQ6L and MRST 2001 LO [35] parton densities, respectively. The shaded bands indicate the maximal possible deviations allowed by the up and down variations along the 20 independent directions that span the 90% confidence level of the data sets entering the CTEQ6 global fit [36].

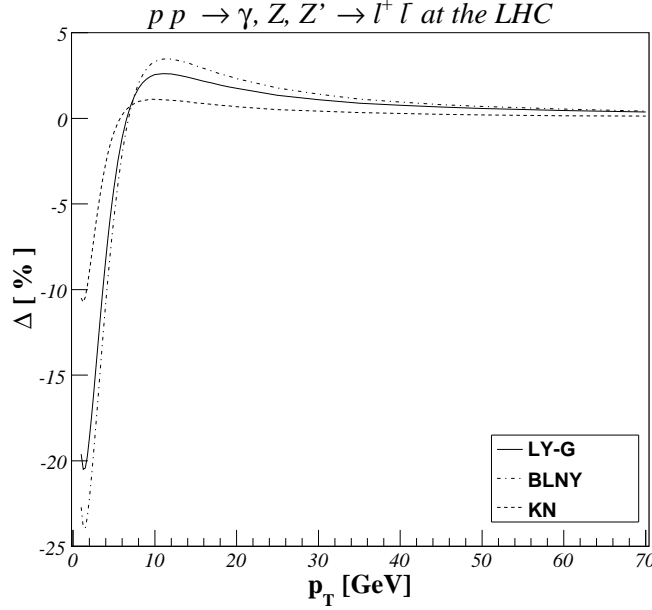


FIG. 8: Variation (in percent) of the transverse-momentum spectrum after matching the NLO QCD corrections to joint resummation with CTEQ6M parton densities for three different choices of a non-perturbative form factor.

and total cross sections in joint p_T and threshold resummation. The two improved predictions were found to be in excellent agreement with each other for mass spectra, p_T spectra, and total cross sections, while the PYTHIA parton and “power” shower predictions usually employed for experimental analyses show significant shortcomings both in normalization and shape. The theoretical uncertainties from scale and parton density variations and non-perturbative effects were found to be 9%, 8%, and less than 5%, respectively, and thus under good control. The implementation of our improved predictions in terms of the new MC@NLO generator or resummed K factors in the analysis chains

of the Tevatron and LHC experiments should be straightforward and lead to more precise determinations or limits of the Z' boson masses and/or couplings. While we have shown numerical results for Z' bosons associated with the $U(1)_\chi$ gauge symmetry, our calculations are completely general and easily applicable to different grand unification, extra-dimensional, or other models. Our modified MC@NLO program has been endorsed by the original authors and can be obtained, like the joint resummation program, at <http://lpsc.in2p3.fr/klasen/software>.

Acknowledgments

This work has been supported by the CNRS/IN2P3 with a pilot grant for the LHC-Theory-France initiative and by two Ph.D. fellowships of the French ministry for education and research. We thank B. Clément for finalizing several figures, D. de Florian for allowing us to use his parton density routines, and S. Frixione for useful comments on the manuscript.

-
- [1] A. Leike, Phys. Rept. **317** (1999) 143.
 - [2] M. Carena, A. Daleo, B. A. Dobrescu and T. M. P. Tait, Phys. Rev. D **70** (2004) 093009.
 - [3] A. Abulencia *et al.* [CDF Collaboration], Phys. Rev. Lett. **96** (2006) 211801.
 - [4] LEP electroweak working group, <http://lepewwg.web.cern.ch>.
 - [5] F. Ledroit, J. Morel and B. Trocme, ATL-PHYS-PUB-2006-024 (July 2006).
 - [6] R. Cousins, J. Mumford and V. Valuev, CMS NOTE 2005/002 (February 2005).
 - [7] T. Sjöstrand, S. Mrenna and P. Skands, JHEP **0605** (2006) 026.
 - [8] C. Ciobanu, T. Junk, G. Veramendi, J. Lee, G. De Lentdecker, K. McFarland and K. Maeshima, FERMILAB-FN-0773-E (July 2005).
 - [9] G. Miu and T. Sjöstrand, Phys. Lett. B **449** (1999) 313.
 - [10] R. Hamberg, W. L. van Neerven and T. Matsuura, Nucl. Phys. B **359** (1991) 343 [Erratum-ibid. B **644** (2002) 403].
 - [11] S. Frixione and B. R. Webber, JHEP **0206** (2002) 029.
 - [12] G. Corcella *et al.*, JHEP **0101** (2001) 010.
 - [13] G. Corcella and M. H. Seymour, Nucl. Phys. B **565** (2000) 227.
 - [14] S. Catani, F. Krauss, R. Kuhn and B. R. Webber, JHEP **0111** (2001) 063.
 - [15] S. Mrenna and P. Richardson, JHEP **0405** (2004) 040.
 - [16] J. Alwall *et al.*, arXiv:0706.2569 [hep-ph].
 - [17] F. Caravaglios, M. L. Mangano, M. Moretti and R. Pittau, Nucl. Phys. B **539** (1999) 215.
 - [18] G. Bozzi, B. Fuks and M. Klasen, arXiv:0709.3057 [hep-ph], Nucl. Phys. B (in press), and references therein.
 - [19] M. B. Green and J. H. Schwarz, Phys. Lett. B **149** (1984) 117.
 - [20] J. L. Hewett and T. G. Rizzo, Phys. Rept. **183** (1989) 193.
 - [21] J. L. Rosner, Phys. Rev. D **35** (1987) 2244.
 - [22] R. W. Robinett and J. L. Rosner, Phys. Rev. D **25** (1982) 3036 [Erratum-ibid. D **27** (1983) 679].
 - [23] P. Abreu *et al.* [DELPHI Collaboration], Phys. Lett. B **485** (2000) 45.
 - [24] P. Aurenche and J. Lindfors, Nucl. Phys. B **185** (1981) 274.
 - [25] G. Bozzi, B. Fuks and M. Klasen, Phys. Rev. D **74** (2006) 015001.
 - [26] G. Bozzi, B. Fuks and M. Klasen, Nucl. Phys. B **777** (2007) 157.
 - [27] H. N. Li, Phys. Lett. B **454** (1999) 328.
 - [28] E. Laenen, G. Sterman and W. Vogelsang, Phys. Rev. D **63** (2001) 114018.
 - [29] A. Kulesza, G. Sterman and W. Vogelsang, Phys. Rev. D **66** (2002) 014011.
 - [30] J. Pumplin, D. R. Stump, J. Huston, H. L. Lai, P. Nadolsky and W. K. Tung, JHEP **0207** (2002) 012.
 - [31] K. Hagiwara *et al.* [Particle Data Group], Phys. Rev. D **66** (2002) 010001.
 - [32] W. M. Yao *et al.* [Particle Data Group], J. Phys. G **33** (2006) 1.
 - [33] S. Frixione and M. L. Mangano, JHEP **0405** (2004) 056.
 - [34] A. D. Martin, R. G. Roberts, W. J. Stirling and R. S. Thorne, Phys. Lett. B **604** (2004) 61.
 - [35] A. D. Martin, R. G. Roberts, W. J. Stirling and R. S. Thorne, Phys. Lett. B **531** (2002) 216.
 - [36] W. K. Tung, H. L. Lai, A. Belyaev, J. Pumplin, D. Stump and C. P. Yuan, JHEP **0702** (2007) 053.
 - [37] G. A. Ladinsky and C. P. Yuan, Phys. Rev. D **50** (1994) 4239.
 - [38] F. Landry, R. Brock, P. M. Nadolsky and C. P. Yuan, Phys. Rev. D **67** (2003) 073016.
 - [39] A. V. Konychev and P. M. Nadolsky, Phys. Lett. B **633** (2006) 710.